

Mechanisms of bandedge emission in Mgdoped ptype GaN

M. Smith, G. D. Chen, J. Y. Lin, H. X. Jiang, A. Salvador et al.

Citation: *Appl. Phys. Lett.* **68**, 1883 (1996); doi: 10.1063/1.116282

View online: <http://dx.doi.org/10.1063/1.116282>

View Table of Contents: <http://apl.aip.org/resource/1/APPLAB/v68/i14>

Published by the [American Institute of Physics](#).

Related Articles

A model for the bandgap energy of the N-rich GaNAs($0 \leq x \leq 0.07$)

Appl. Phys. Lett. **100**, 142112 (2012)

Defect evolution and interplay in n-type InN

Appl. Phys. Lett. **100**, 091907 (2012)

Assessment of deep level defects in m-plane GaN grown by metalorganic chemical vapor deposition

Appl. Phys. Lett. **100**, 082103 (2012)

Deep traps in nonpolar m-plane GaN grown by ammonia-based molecular beam epitaxy

Appl. Phys. Lett. **100**, 052114 (2012)

The influence of Al composition on point defect incorporation in AlGaIn

Appl. Phys. Lett. **100**, 043509 (2012)

Additional information on *Appl. Phys. Lett.*

Journal Homepage: <http://apl.aip.org/>

Journal Information: http://apl.aip.org/about/about_the_journal

Top downloads: http://apl.aip.org/features/most_downloaded

Information for Authors: <http://apl.aip.org/authors>

ADVERTISEMENT



PFEIFFER  **VACUUM**

Complete Dry Vacuum Pump Station
for only **\$4995** — HiCube™ Eco

800-248-8254 | www.pfeiffer-vacuum.com

Mechanisms of band-edge emission in Mg-doped *p*-type GaN

M. Smith, G. D. Chen,^{a)} J. Y. Lin, and H. X. Jiang
Department of Physics, Kansas State University, Manhattan, Kansas 66506-2602

A. Salvador, B. N. Sverdlov, A. Botchkarev, and H. Morkoc^{b)}
Materials Research Laboratory and Coordinated Science Laboratory, University of Illinois at Urbana-Champaign, Urbana, Illinois 61801

B. Goldenberg
Honeywell Technology Center, Plymouth, Minnesota 55441

(Received 21 November 1995; accepted for publication 26 January 1996)

Time-resolved photoluminescence has been employed to study the mechanisms of band-edge emissions in Mg-doped *p*-type GaN. Two emission lines at about 290 and 550 meV below the band gap (Eg) have been observed. Their recombination lifetimes, dependencies on excitation intensity, and decay kinetics have demonstrated that the line at 290 meV below Eg is due to the conduction band-to-impurity transition involving shallow Mg impurities, while the line at 550 meV below Eg is due to the conduction band-to-impurity transition involving doping related deep-level centers (or complexes). © 1996 American Institute of Physics. [S0003-6951(96)00614-0]

The recent progress in GaN based devices including efficient blue light emitting diodes (LEDs) has demonstrated its potential. However, many aspects of the basic properties of GaN and related semiconductors remain to be understood and improved. As is well known, presently *p*-type GaN doping is achieved more readily with Mg impurities.¹ Moreover, Mg doping renders the as-grown GaN by metalorganic chemical vapor deposition (MOCVD) highly resistive. A post-growth thermal annealing in a nitrogen ambient is required to activate the Mg dopants in order to obtain *p*-type conduction, possibly due to the dissociation of H–Mg complexes.² Only recently, as-deposited *p*-type doping GaN has been achieved by molecular beam epitaxy (MBE) without post-growth treatment,^{3–5} which has tentatively been attributed to the absence of H in MBE growth. While recent Hall measurements indicate that Mg acceptors in *p*-type GaN have a thermal activation energy of about 160 meV,⁶ the dominant emission line in current commercially available blue LEDs based on Mg-doped GaN is around 430–450 nm at room temperature, which is about 550 meV below the band gap.

Previously we have employed time-resolved photoluminescence (PL) to study the optical transitions of free A- and B-excitons (AX at ~3.483 eV and BX at ~3.489 eV), neutral-donor-bound excitons (I_2 at ~3.475 eV), and neutral-acceptor-bound excitons (I_1 at ~3.459 eV) and their dynamic processes in GaN.^{7,8} Our results have demonstrated that time-resolved PL is a powerful technique for elucidating mechanisms of optical transitions. In this work we have applied the same technique to study the mechanisms of band-edge emissions in Mg-doped *p*-type GaN. Both MBE and MOCVD grown samples have been investigated. We have observed, independent of growth methods, two broad emission bands at about 290 and 550 meV below the band gap (Eg) that dominate, respectively, at low ($T < 150$ K) and high

temperatures ($T > 150$ K). PL temporal behaviors have shown that the band-to-impurity transitions, involving shallow Mg acceptors at low temperatures ($T < 150$ K) and Mg doping induced deep centers (or complexes) at higher temperatures ($T > 150$ K), are the dominant recombination processes in relatively heavily doped *p*-GaN under our experimental conditions.

The *P*-type GaN epitaxial layers (thicknesses vary from 2 to 5 μm) used here were grown by MBE and MOCVD on sapphire (Al_2O_3) substrates with 50 nm AlN buffer layers. For MOCVD grown layers, the Mg-doped as-grown material was a high resistivity *p*-type. Post-growth thermal annealing in flowing nitrogen at 76 Torr and 750 °C for about 20 min was employed to activate the Mg impurities. Time-resolved PL spectra were measured by using a picosecond laser spectroscopy system with an average output power of about 20 mW and a tunable photon energy up to 4.5 eV.^{7,8}

Figure 1 presents typical continuous-wave (cw) PL spectra of *p*-type GaN layers at three representative temperatures. The arrows indicate peak positions at different temperatures. At 10 K one dominant emission band at about 3.21 eV is seen, which is almost absent at $T > 150$ K. The I_1 line at about 3.46 eV is also clearly observable at low temperatures. There is also an additional weak emission band at a lower energy position (~2.95 eV), which dominates at higher temperatures, $T > 150$ K. Recall that the band gap variation with temperature is only about 20 meV in the region $10 \text{ K} < T < 150 \text{ K}$. The spectral peak positions of the observed emission bands have also been measured under different excitation intensities. The peak positions shifted toward higher emission energies as the excitation intensity was increased. Finally, the peak position of the lower energy emission line also shifts toward lower energies as the doping concentration increases (not shown). At room temperature, the peak position of this lower energy emission band can be varied from 430 to 490 nm. As an example, the room-temperature emission spectra obtained at two different excitation intensities are shown in the inset of Fig. 1 with H I_{exc} and L I_{exc} denoting, respectively, the high and low excitation intensities,

^{a)}Permanent address: Department of Applied Physics, Xi'an Jiaotong University, P. R. China.

^{b)}On sabbatical at Wright Laboratory under a University Resident Research Program sponsored by AFOSR.

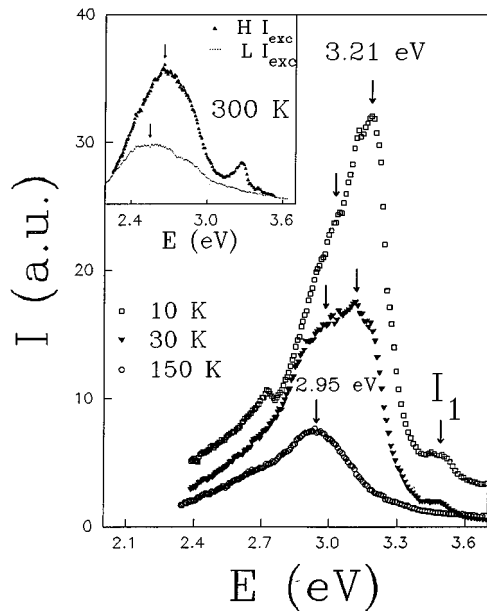


FIG. 1. Continuous wave photoluminescence (PL) spectra measured at three representative temperatures for Mg-doped *p*-GaN samples, which show a dominant emission line at about 3.21 eV at low temperatures. Another lower energy emission line at about 2.95 eV ($T=10$ K) dominates at higher temperatures ($T>150$ K). The inset shows the room-temperature PL spectra associated with the lower energy emission band obtained for higher excitation ($H I_{exc}$) and lower excitation intensities ($L I_{exc}$), showing that the spectral peak position shifts toward higher energies as the excitation intensity increases.

which differ by a factor of about 3. A blueshift in the peak position with increasing excitation intensity can be seen clearly. This lower energy emission band has been observed previously in MOCVD grown and post-growth thermal annealed *p*-GaN films² and is being utilized for violet-blue emission in *p-n* junction GaN LEDs.^{9,10}

In order to explore the physical origin of the observed emission lines, their dynamical behaviors have been studied. Figure 2(a) shows an example of the PL temporal response of the 3.21 eV band measured at 10 K. At low temperatures, PL decay is nonexponential, but can be approximated by two exponential decay as illustrated by the solid fitting curve in Fig. 2(a). At 10 K, the typical lifetime of the fast component which contributes 87% of the PL signal is about 0.6 ns and the slow component is about 5.0 ns. The temperature dependence of the recombination lifetime of the fast (major) PL component of the 3.21 eV line is shown in the inset of Fig. 2(a). In the temperature region $T<150$ K where the 3.21 eV emission band dominates, the recombination lifetime decreases progressively from 0.6 to 0.3 ns as temperature increases from 10 to 140 K. This behavior can be accounted for by an increased nonradiative recombination rate at higher temperatures. This is consistent with the observation of the thermal quenching of the 3.21 eV emission line and the subsequent increase in the emission intensity of the lower energy band at 2.95 eV with temperature as seen in Fig. 1. However, the lifetime of 0.6 ns obtained at 10 K should represent the radiative recombination lifetime of the 3.21 eV emission band.

In the higher temperature region ($T>150$ K), where the lower energy emission band (~ 2.95 eV at $T<150$ K) domi-

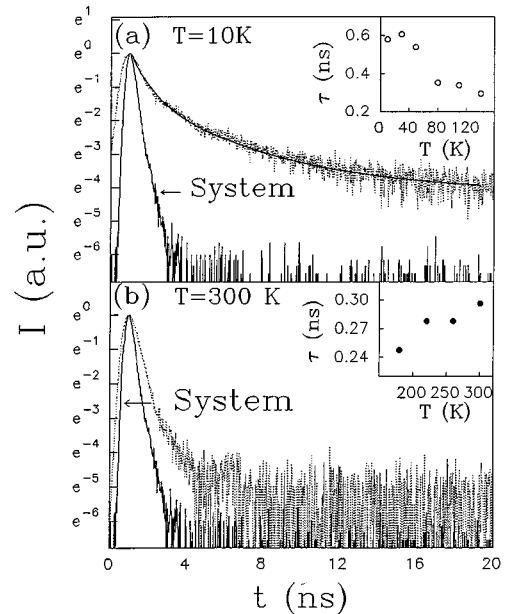


FIG. 2. (a) Temporal responses of the 3.21 eV emission band measured at $T=10$ K and (b) 2.95 eV emission band measured at room temperature. The solid lines are the least-squares fit of data with two exponential decay, $I(t)=I_1 \exp(-t/\tau_1)+I_2 \exp(-t/\tau_2)$. The fast decay component contributes 87% and 97% of the PL signal at 10 and 300 K, respectively. The insets of (a) and (b) show the temperature dependencies of the recombination lifetimes for higher energy emission line (the fast decay component) and the lower energy emission band (around 2.6 eV at $T=300$ K), respectively.

nates, the fast decay component contributes nearly 97% of the PL signal and consequently the decay kinetics of PL is nearly single exponential. This is illustrated in Fig. 2(b), in which a PL temporal response measured at the corresponding spectral peak position is shown for 300 K. Also shown in the inset of Fig. 2(b) is the temperature dependence of the recombination lifetime of the lower energy emission band, which indicates that its lifetime increases slightly with temperature. This is due to the carrier transformation from the 3.21 eV recombination channel as discussed above.

The observed subnanosecond PL recombination lifetimes suggest that the band-edge emissions in Mg-doped *p*-GaN result predominantly from the conduction band-to-impurity recombination, involving substitutional shallow Mg acceptors at low temperatures ($T<150$ K) and deep-level centers at high temperatures ($T>150$ K). In such a context, the quenching of the 3.21 eV emission line is due to the processes of either thermal ionization of shallow neutral Mg acceptors or hole transfer from the shallow to the deep impurities or complexes as temperature increases.

A previous work on band-to-impurity transitions involving a donor and the valence band has shown that this type of transition in *n*-type GaN samples of a similar impurity concentration has a typical recombination lifetime between 0.3–0.7 ns depending on the impurity binding energy,¹¹ which further corroborate our assignment here. On the other hand, the properties of donor-to-acceptor pair (DAP) transitions in GaN have also been investigated rather thoroughly in a previous work,¹² which showed that the DAP transitions in GaN have recombination lifetimes on the order of a few microseconds. This is also fairly typical in well understood semiconductors such as CdS.¹³ These seem to suggest again that the

transitions observed are not of a DAP nature. Furthermore, the emission peak positions shift toward higher energies as the excitation intensity increases, as illustrated in the inset of Fig. 1. We have observed a similar blueshift for the 3.21 eV emission band at low temperatures. However, the blueshift is much more pronounced for the lower energy band at higher temperatures, suggesting a deep-level impurity band formation, most likely caused by heavy doping. Thus an increase in excitation intensity not only increases the quasi-Fermi level for the electrons in the conduction band, but also sweeps the quasi-Fermi level for holes within the impurity band to a higher position. If the transitions were DAP-like, the electrons would leak out of the conduction band through the donors and the quasi-Fermi level for electrons would not affect the emission spectrum significantly.¹⁴ As another point, we note that the line shapes seen here are quite similar for different delay times due to the broadness of the emission band and the shortness of recombination lifetimes. This is depicted in Fig. 3, where we have plotted the time-resolved emission spectra for the 3.21 eV band at $T=10$ K. The emission spectral line shape of a DAP transition is expected to be delay time dependent with a much larger time scale for delay times. Finally, based on a theoretical model developed by Avouris and Morgan,¹⁵ the decay kinetics of both the band-to-impurity and DAP recombination are not necessarily exponential. The asymptotic decay at longer times was predicted to follow t^{-1} for the DAP recombination. The decay of the band-to-impurity recombination at longer times should follow t^α with α being larger than 1, because the product of the time variations of the free carriers and the DAP recombination gives the decay of the band-to-impurity recombination. In the inset of Fig. 3, we have plotted the 10 K PL temporal response obtained at the spectral peak position in a double logarithmic scale, which clearly shows that the decay at longer delay times following a power law with an exponent close to 1.4, which further suggests that the dominant emission lines are of a band-to-impurity nature.

Our results suggest an optical ionization energy of about 290 meV for the shallow Mg acceptors and 550 meV for doping induced deep centers (or complexes). The discrepancy between the thermal ionization energy (160 meV) and the optical ionization energy (290 meV) of the shallow Mg acceptors may be accounted for by a lattice relaxation associated with doped impurities in GaN, and effect that is rather common in other wide band gap semiconductors. The observed subnanosecond radiative recombination lifetimes of the band-to-impurity recombination can also explain the high photoluminescence quantum yield associated with the emission lines seen in p -type GaN samples.

In conclusion, time-resolved PL spectroscopy has been employed to study the mechanisms of band-edge emissions in Mg-doped p -type GaN grown both by MOCVD and MBE. Two emission lines at about 290 and 550 meV below E_g have been observed. Their recombination lifetimes, dependencies on excitation intensity, and decay kinetics have demonstrated that the line at 290 meV below the band gap is due to the conduction band-to-impurity transition involving shallow Mg impurities, while the line at 550 meV below the band gap is due to the conduction band-to-impurity transition

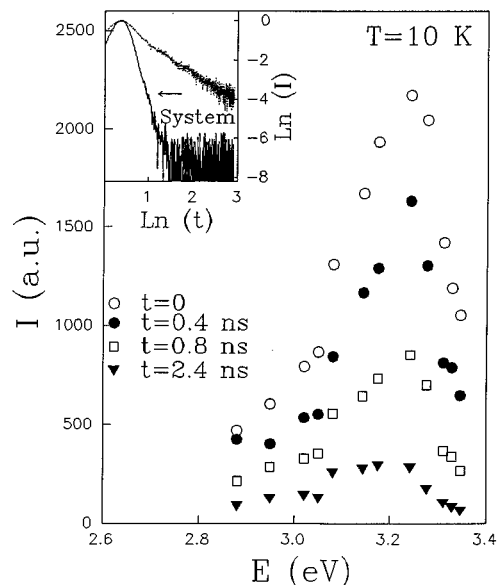


FIG. 3. Time-resolved emission spectra of the 3.21 eV emission band measured at $T=10$ K. The delay time t is measured with respect to the peak positions of the temporal responses such as those shown in Fig. 2. The inset shows a logarithmic plot of the low-temperature ($T=10$ K) PL temporal response measured at the spectral peak position 3.21 eV, which shows that the PL decay at longer times is described by a power law, $I(t) \sim I_0 t^{-\alpha}$ ($t \gg t_0$ with $t_0 \approx 0.5$ ns) with α close to 1.4.

involving doping related deep-level impurities (or complexes).

J.Y.L. and H.X.J. would like to thank Dr. John Zavada for insightful discussions and encouragement. A.S., B.S., A.B., and H.M. would like to acknowledge the support of the ONR and thank Max Yoder and Dr. Y. S. Park for monitoring the program. H.M. acknowledges valuable discussions with Dr. Zook and Professor Paul Ruden.

- ¹H. Morkoc, S. Strite, G. B. Gao, M. E. Lin, B. Sverdlov, and M. Burns, *J. Appl. Phys.* **76**, 1363 (1994).
- ²S. Nakamura, N. Iwasa, M. Senoh, and T. Mukai, *Jpn. J. Appl. Phys.* **31**, 1258 (1992); S. Nakamura, M. Senoh, and T. Mukai, *ibid.* **32**, L8 (1993).
- ³M. S. Brandt, N. M. Johnson, R. J. Molnar, R. Singh, and T. D. Moustakas, *Appl. Phys. Lett.* **64**, 2264 (1994).
- ⁴M. Rubin, N. Newman, J. S. Chan, T. C. Fu, and J. R. Ross, *Appl. Phys. Lett.* **64**, 64 (1994).
- ⁵M. E. Lin, G. Xue, G. L. Zhou, J. E. Green, and H. Morkoc, *Appl. Phys. Lett.* **63**, 932 (1993).
- ⁶T. Tanaka, A. Watanabe, A. Amano, Y. Kobayashi, I. Akasaki, S. Yamazaki, and M. Koike, *Appl. Phys. Lett.* **65**, 593 (1994).
- ⁷M. Smith, G. D. Chen, J. Z. Li, J. Y. Lin, H. X. Jiang, A. Salvador, W. K. Kim, O. Aktas, A. Botchkarev, and H. Morkoc, *Appl. Phys. Lett.* **67**, 3387 (1995).
- ⁸G. D. Chen, M. Smith, J. Y. Lin, H. X. Jiang, M. Asif Khan, and C. J. Sun, *Appl. Phys. Lett.* **67**, 1653 (1995); M. Smith, G. D. Chen, J. Y. Lin, H. X. Jiang, M. Asif Khan, and C. J. Sun, *ibid.* **67**, 3295 (1995).
- ⁹B. Goldenberg, J. D. Zook, and R. Ulmer, *Appl. Phys. Lett.* **62**, 381 (1993).
- ¹⁰I. Akasaki, H. Amano, M. Kito, and K. Hiramatsu, *J. Lumin.* **48/49**, 666 (1991).
- ¹¹M. Smith, G. D. Chen, J. Y. Lin, H. X. Jiang, A. Salvador, B. N. Sverdlov, A. Botchkarev, and H. Morkoc, *Appl. Phys. Lett.* **66**, 3477 (1995).
- ¹²R. Dingle and M. Ilegems, *Solid State Commun.* **9**, 175 (1971).
- ¹³D. G. Thomas, J. J. Hopfield, and W. M. Augustyniak, *Phys. Rev.* **140**, 202 (1965).
- ¹⁴J. I. Pankove, *Optical Processes in Semiconductors* (Dover, New York, 1971), Chap. 6, p. 148.
- ¹⁵P. Avouris and T. N. Morgan, *J. Chem. Phys.* **74**, 4347 (1981).